New Phytologist

Research

Deciphering the variability of leaf phosphorus-allocation strategies using leaf economic traits and reflectance spectroscopy across diverse forest types

Tingting Dong[1,2,3], Fengqi Wu[1,2,3], Yuki Tsujii[4], Philip A. Townsend[5], Nan Yang[1,2,3], Weiying Xu[1,2,3], Shuwen Liu[6,7], Nathan G. Swenson[8], Julien Lamour[9], Wenxuan Han[10], Nicholas G. Smith[11], Yue Shi[1,2,3], Li Yan[12], Di Tian[13], Mingkai Jiang[14], Zhihui Wang[15], Xiaojuan Liu[1,2,3], Guanhua Dai[16], Jinlong Dong[3,17,18], Jordi Sardans[19,20], Peter B. Reich[21,22,23], Hans Lambers[12,24], Shawn P. Serbin[25], Josep Peñuelas[19,20], Jin Wu[6,26,27] and Zhengbing Yan[1,2,3]

[1]State Key Laboratory of Forage Breeding-by-Design and Utilization, Key Laboratory of Vegetation and Environmental Change, Institute of Botany, Chinese Academy of Sciences, Xiangshan, Beijing, 100093, China; [2]China National Botanical Garden, Beijing, 100093, China; [3]University of Chinese Academy of Sciences, Yuquanlu, Beijing, 100049, China; [4]Forestry and Forest Products Research Institute, Tsukuba, 305-8687, Japan; [5]Department of Forest & Wildlife Ecology, University of Wisconsin-Madison, Madison, WI 53706, USA; [6]School of Biological Sciences, The University of Hong Kong, Hong Kong, 999077, China; [7]Department of Forest and Wildlife Ecology, University of Wisconsin-Madison, 1630 Linden Drive, Madison, WI 53706, USA; [8]Department of Biological Sciences, University of Notre Dame, Notre Dame, IN 46565, USA; [9]Centre de Recherche sur la Biodiversité et l'Environnement (CRBE), Université de Toulouse, CNRS, IRD, Toulouse INP, Université Toulouse 3 – Paul Sabatier (UT3), Toulouse, 31062, France; [10]Key Laboratory of Plant-Soil Interactions, Ministry of Education, College of Resources and Environmental Sciences, China Agricultural University, Beijing, 100193, China; [11]Department of Biological Sciences, Texas Tech University, Lubbock, TX 79409, USA; [12]School of Biological Sciences, University of Western Australia, Perth, WA, 6009, Australia; [13]State Key Laboratory of Efficient Production of Forest Resources, Beijing Forestry University, Beijing, 100083, China; [14]College of Life Sciences, Zhejiang University, Hangzhou, 310058, China; [15]Guangdong Provincial Key Laboratory of Remote Sensing and Geographical Information System, Guangdong Open Laboratory of Geospatial Information Technology and Application, Guangzhou Institute of Geography, Guangdong Academy of Sciences, Guangzhou, 510070, China; [16]Research Station of Changbai Mountain Forest Ecosystems, Chinese Academy of Sciences, Antu, 133613, China; [17]CAS Key Laboratory of Tropical Forest Ecology, Xishuangbanna Tropical Botanical Garden, Chinese Academy of Sciences, Mengla, Menglun, 666303, China; [18]National Forest Ecosystem Research Station at Xishuangbanna, Xishuangbanna Tropical Botanical Garden, Chinese Academy of Sciences, Mengla, Menglun, 666303, Yunnan, China; [19]CSIC, Global Ecology Unit CREAF-CSIC-UAB, Bellaterra, Barcelona, Catalonia, 08193, Spain; [20]CREAF, Cerdanyola del Vallès, Barcelona, Catalonia, 08193, Spain; [21]Hawkesbury Institute for the Environment, Western Sydney University, Locked Bag 1797, Penrith, NSW, 2751, Australia; [22]Department of Forest Resources, University of Minnesota, St Paul 55108 MN, USA; [23]Institute for Global Change Biology, and School for the Environment and Sustainability, University of Michigan, Ann Arbor, MI 48109, USA; [24]School of Grassland Science, Beijing Forestry University, Beijing, 100083, China; [25]Biospheric Sciences Laboratory, NASA Goddard Space Flight Center, Greenbelt, MD 20771, USA; [26]Institute for Climate and Carbon Neutrality, The University of Hong Kong, Hong Kong, 999077, China; [27]State Key Laboratory of Agrobiotechnology, Chinese University of Hong Kong, Hong Kong, 999077, China

Author for correspondence:
Zhengbing Yan
Email: zbyan@ibcas.ac.cn

Received: *11 December 2024*
Accepted: *27 April 2025*

New Phytologist (2025) **247:** 1129–1144
doi: 10.1111/nph.70219

Key words: leaf economics spectrum, leaf P fractions, leaf reflectance spectroscopy, nutrient limitation, photosynthesis, plant functional traits, plant P-use strategy.

Summary

• Allocation of leaf phosphorus (P) among different functional fractions represents a crucial adaptive strategy for optimizing P use. However, it remains challenging to monitor the variability in leaf P fractions and, ultimately, to understand P-use strategies across diverse plant communities.

• We explored relationships between five leaf P fractions (orthophosphate P, P_i; lipid P, P_L; nucleic acid P, P_N; metabolite P, P_M; and residual P, P_R) and 11 leaf economic traits of 58 woody species from three biomes in China, including temperate, subtropical and tropical forests. Then, we developed trait-based models and spectral models for leaf P fractions and compared their predictive abilities.

• We found that plants exhibiting conservative strategies increased the proportions of P_N and P_M, but decreased the proportions of P_i and P_L, thus enhancing photosynthetic P-use efficiency, especially under P limitation. Spectral models outperformed trait-based models in predicting cross-site leaf P fractions, regardless of concentrations (R^2 = 0.50–0.88 vs 0.34–0.74) or proportions (R^2 = 0.43–0.70 vs 0.06–0.45).

• These findings enhance our understanding of leaf P-allocation strategies and highlight reflectance spectroscopy as a promising alternative for characterizing large-scale leaf P fractions and plant P-use strategies, which could ultimately improve the physiological representation of the plant P cycle in land surface models.

Introduction

Phosphorus (P) is an essential element for plant growth (Sterner & Elser, 2002; White & Hammond, 2008; Hawkesford *et al.*, 2022), often constraining plant productivity in many terrestrial ecosystems (Elser *et al.*, 2007; Vitousek *et al.*, 2010; Du *et al.*, 2020). Understanding how plants adapt to varying environmental conditions is a central theme in plant ecology and biogeochemistry (Vitousek *et al.*, 2010). A key aspect of this is to decipher how leaf P is allocated among different functional fractions. Typically, leaf P exists as free inorganic orthophosphate (P_i) and organic phosphate esters (P_o). A minimal quantity of metabolically active P_i is distributed in the cytoplasm (Bieleski, 1968; Mimura *et al.*, 1996), while excess P_i is stored in vacuoles as a buffer to regulate P_i levels in the cytoplasm (Hooda & Weston, 1999; Ostertag, 2010). P_o can be further divided into four major fractions: lipid P (P_L), nucleic acid P (P_N), metabolite P (P_M) and residual P (P_R) (Chapin & Kedrowski, 1983; Hidaka & Kitayama, 2011; Yan *et al.*, 2019). P_L represents a significant component of the cellular membrane system, particularly the endoplasmic reticulum (Lagace & Ridgway, 2013; Lambers, 2022). P_N comprises nucleic acids (Veneklaas *et al.*, 2012; Suriyagoda *et al.*, 2022), playing a role in the synthesis and turnover of proteins (Veneklaas *et al.*, 2012; Lambers, 2022). P_M encompasses various low-molecular-weight metabolites, including ribulose-1,5-bisphosphate, NADP, ATP, adenosine diphosphate (ADP), sugar phosphates and storage compounds like phytate (Yan *et al.*, 2019; Suriyagoda *et al.*, 2022; Tsujii *et al.*, 2023, 2024). By contrast, the function of major P_R components remains unclear, aside from phosphorylated proteins (Kedrowski, 1983; Lambers *et al.*, 2012). Collectively, exploring the trade-off among different functional leaf P fractions is crucial for deciphering plant P-use strategies.

The concentrations (here denoted as $[P_i]$, $[P_L]$, $[P_N]$, $[P_M]$ and $[P_R]$) and relative proportions (here denoted as rP_i, rP_L, rP_N, rP_M and rP_R) of leaf P fractions vary substantially across plant species and soil nutrient availability (Lambers, 2022; Suriyagoda *et al.*, 2022; Tsujii *et al.*, 2024; Meng *et al.*, 2025). Species in low-P soils always have low concentrations of total leaf P, often with low $[P_i]$, $[P_N]$ and $[P_L]$ (Hidaka & Kitayama, 2011; Mo *et al.*, 2019; Yan *et al.*, 2019; Tsujii *et al.*, 2024). These likely reflect the depletion of P_i storage in vacuoles (White & Hammond, 2008), low levels of rRNA (Sulpice *et al.*, 2014) and substitution of phospholipids by P-free lipids (Lambers *et al.*, 2012), respectively. By contrast, $[P_M]$ and $[P_R]$ are invariant or slightly lower in lower-P soils. Considering the pattern of the proportions of leaf P fractions, there is no definitive conclusion in Borneo (Hidaka & Kitayama, 2011) or in Australia (Yan *et al.*, 2019; S. T. Liu *et al.*, 2023; Tsujii *et al.*, 2023, 2024). Even more, species-dependent patterns characterized the proportions of leaf P fractions among 18 woody species (Yan *et al.*, 2019) and among three woody species (S. T. Liu *et al.*, 2023) in Western Australia. However, it is unclear whether these findings apply to species world-wide, as many previous studies focused on species from P-impoverished soils and limited plant communities (Hidaka & Kitayama, 2011; Yan *et al.*, 2019; S. T. Liu *et al.*, 2023; Tsujii *et al.*, 2023, 2024). The chemical assays for determining leaf P fractions are time-consuming and labor-intensive. This may lead to inadequate spatial coverage of leaf P fractions, thus hindering the characterization of the patterns of leaf P fractions across diverse forest communities.

Empirical leaf trait relationships are often used to indirectly infer important but difficult-to-measure traits (e.g. leaf life span, leaf maximum carboxylation rate of the enzyme RuBisCO ($V_{c,max}$) and leaf dark respiration) from more easily measurable ones (e.g. specific leaf area (SLA), leaf nitrogen (N) concentration ([N]), leaf Chl concentration ([Chl])) (Reich *et al.*, 2007; Croft *et al.*, 2017; Z.B. Yan *et al.*, 2021; Wu *et al.*, 2025). A typical example of this is the well-established leaf economics spectrum (LES), which illustrates that light-saturated net photosynthetic rate (A_{sat}) is positively correlated with [N] and SLA. These correlations represent core components of the LES, which encapsulates plant growth and adaptive strategies ranging from conservative to acquisitive resource use strategies (Lambers & Poorter, 1992; Reich *et al.*, 1997; Westoby *et al.*, 2002; Wright *et al.*, 2004). Indeed, empirical studies have shown that leaf P fractions are related to LES traits (Hidaka & Kitayama, 2011, 2013; S. T. Liu *et al.*, 2023; Tsujii *et al.*, 2023, 2024). Specifically, [N] shows a positive correlation with $[P_N]$ and $[P_R]$, while negatively correlating with rP_L (Hidaka & Kitayama, 2011; Tsujii *et al.*, 2024), highlighting the role of P in the synthesis and turnover of proteins (Thornley & Cannell, 2000; Veneklaas *et al.*, 2012). Given that P is crucial for photosynthetic processes, A_{sat} is positively correlated with the concentrations of the five P fractions (Hidaka & Kitayama, 2013; Zhang *et al.*, 2018; Tsujii *et al.*, 2023). Specific leaf area also exhibits a significant positive correlation with the concentrations of leaf P fractions (Hidaka & Kitayama, 2011, 2013; Tsujii *et al.*, 2024). Interestingly, Tsujii *et al.* (2024) found a negative correlation between SLA and rP_L, suggesting that, as SLA decreases, ecological strategies shift toward allocating more leaf P to membrane structures. Consequently, leaf P fractions can potentially be inferred from these leaf trait correlations. Moreover, the LES offers valuable insights into plant P-use strategies (Hidaka & Kitayama, 2013; Lambers, 2022). Although the associations between leaf economic traits and P fractions are apparent, standard models have yet to be developed to predict the variability in leaf P fractions across forest communities from diverse climate zones.

While empirical relationships among leaf traits hold great potential for predicting leaf P fractions across diverse forest

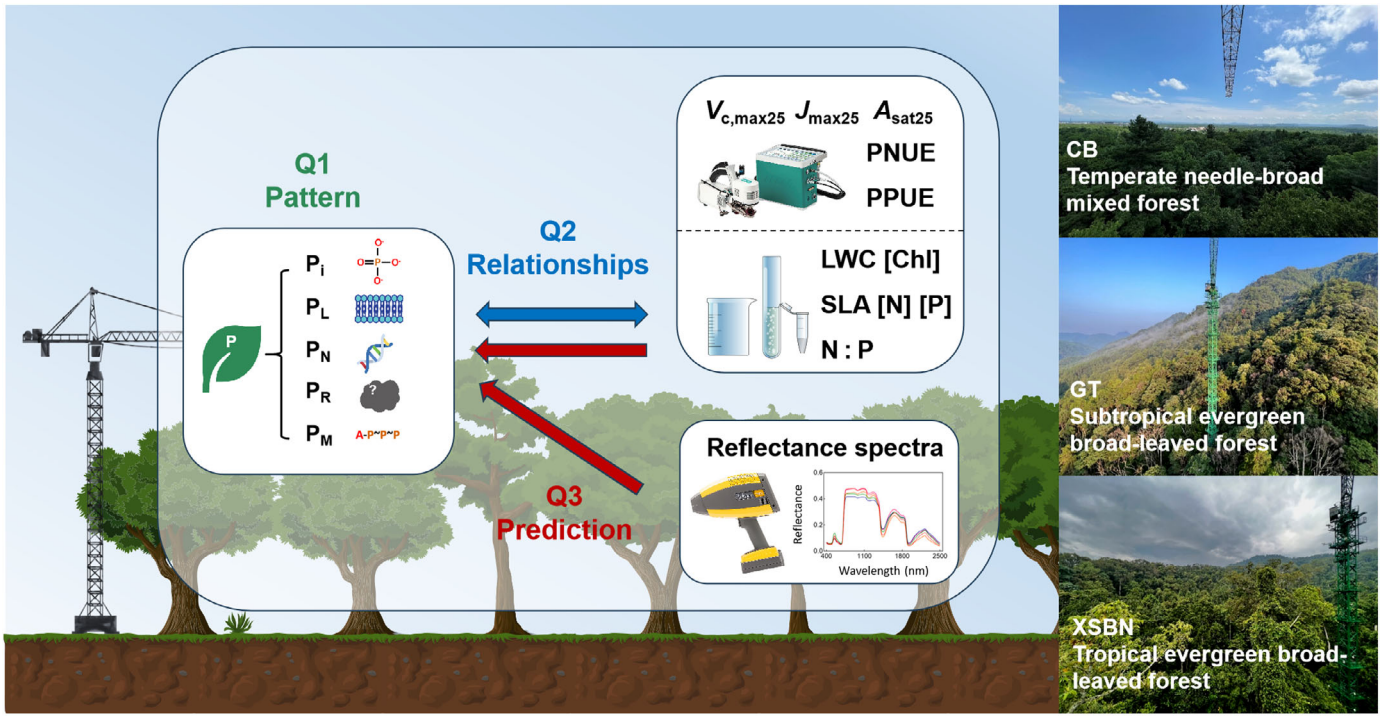

Fig. 1 Conceptual diagram illustrating the goals of this study. This study was conducted at three sites in China, including a temperate forest at Changbai Mountain (CB), a subtropical forest at Gutian Mountain (GT) and a tropical forest at Xishuangbanna (XSBN). At each forest site, the Chinese Academy of Sciences maintains a canopy crane, shown in the three pictures in panels on the right. This study aimed to address three questions: (1) Question 1 (Q1): how do leaf phosphorus (P) fractions vary across diverse forest types? (2) Q2: what are the relationships between leaf P fractions and economic traits? (3) Q3: can leaf reflectance spectroscopy provide an efficient alternative to predict leaf P fractions compared with empirical leaf trait correlations? [Chl], leaf Chl concentration; [N], leaf N concentration; [P], leaf P concentration; A_{sat25}, light-saturated net photosynthetic rate standardized to 25°C; J_{max25}, the maximum electron transport rate standardized to 25°C; LWC, leaf water content; N : P, N to P ratio; P_i, orthophosphate P; P_L, lipid P; P_M, metabolite P; P_N, nucleic acid P; PNUE, photosynthetic N-use efficiency; PPUE, photosynthetic P-use efficiency; P_R, residual P; SLA, specific leaf area; $V_{c,max25}$, the maximum carboxylation rate of the enzyme RuBisCO standardized to 25°C.

communities, there are sampling difficulties associated with accessing the canopy to collect species representative of the entire community. Leaf reflectance spectroscopy may provide a fast and efficient means for monitoring leaf traits based on optical properties, thus reducing the burden of *in situ* leaf sampling and traditional chemical assays (Serbin & Townsend, 2020; Kothari *et al.*, 2023b). The underlying biophysical principle is that various leaf compounds, including pigments, proteins, lignin and cellulose, exhibit light absorption features at specific wavelengths (Curran, 1989; Elvidge, 1990; Kokaly *et al.*, 2009). The tight connections of leaf reflectance spectra to morphological, biochemical and physiological properties (Curran, 1989; Ollinger, 2011; Féret *et al.*, 2017, 2019; Serbin & Townsend, 2020), combined with the high resolution of spectroradiometers (400–2500 nm, < 10 nm spectral resolution), enable estimating plant traits at a geographic scale that is difficult to achieve for traditional chemical assays (Wang *et al.*, 2022). Indeed, spectroscopy has proven effective in estimating a broad suite of leaf morphological and biochemical traits related to leaf P fractions, including SLA (Serbin *et al.*, 2019; Kothari *et al.*, 2023a), leaf water content (LWC; Z.B. Yan *et al.*, 2021), [Chl] (Asner *et al.*, 2014; Wijewardane *et al.*, 2023) and [N] (Chen *et al.*, 2022; S. W. Liu *et al.*, 2023). Furthermore, although no major spectral absorption features are associated with P chemical bonds in the 400–2500 nm range, leaf total P concentration ([P]) has been accurately predicted by leaf reflectance (Asner *et al.*, 2014; Chen *et al.*, 2022; Wijewardane *et al.*, 2023; Kothari *et al.*, 2023a; Gill *et al.*, 2024), based on P-related traits detectable via spectroscopy. These results suggest that spectroscopy can provide an alternative approach to characterize the variability in leaf P fractions. As data volumes increase, leaf-level spectral-trait models demonstrate broad spatial generalizability, enabling a single spectra-trait model to be applied over large spatial scales (Martin *et al.*, 2008; Asner *et al.*, 2014; Serbin *et al.*, 2019; Z.B. Yan *et al.*, 2021), which provides the potential to expand the spatial coverage of leaf P fractions. There is a knowledge gap concerning whether leaf reflectance spectra can accurately predict leaf P fractions across diverse forest communities, highlighting the need for further investigation.

This study aimed to elucidate plant P-use strategies across diverse forest communities, as well as to explore whether leaf reflectance spectroscopy can address data gaps of leaf P fractions (Fig. 1). Specifically, we addressed three questions:

(**1**) How do leaf P fractions vary across diverse forest types?

(**2**) What are the relationships between leaf P fractions and economic traits?

(3) Can leaf reflectance spectroscopy provide an efficient alternative to predict leaf P fractions compared with empirical leaf trait correlations?

To address these questions, we collected leaf samples of canopy trees from three diverse forest types, including a temperate needle-and-broad-leaved mixed forest, a subtropical evergreen broad-leaved forest and a tropical evergreen broad-leaved forest. Using these samples, we measured the concentrations and proportions of leaf P fractions, 11 leaf traits (i.e. SLA, LWC, [Chl], [N], [P], leaf N to P ratio (N : P), $V_{c,max}$, the maximum electron transport rate (J_{max}), A_{sat}, photosynthetic P-use efficiency (PPUE) and photosynthetic N-use efficiency (PNUE)) and leaf reflectance spectra. By answering these questions, we hope to provide a practical approach for capturing the variability in leaf P fractions, thereby deepening our understanding of plant P-use strategies across plant species and growth conditions.

Materials and Methods

Study sites and plant sampling

This study was conducted at three forests in China, including a temperate needle-and-broad-leaved mixed forest at Changbai Mountain (temperate mixed forest CB; 42°23′N, 128°05′E), a subtropical evergreen broad-leaved forest at Gutian Mountain (subtropical evergreen forest GT; 29°15′N, 118°07′E) and a tropical evergreen broad-leaved forest at Xishuangbanna (tropical evergreen forest XSBN; 21°37′N, 101°34′E). These sites were selected for two main reasons. First, each forest is equipped with a canopy crane operated by the Chinese Academy of Sciences, allowing easy access to the upper canopy tree species representative of each forest community. Second, these sites represent typical forest types in China (i.e. temperate, subtropical and tropical forests) and span large environmental gradients, therefore ensuring a sufficient breadth of leaf P fractions, leaf traits and reflectance spectra. Specially, the mean annual temperature (MAT) and mean annual precipitation (MAP) vary significantly across the sites (2.8°C and 691 mm at temperate mixed forest CB, 15.3°C and 1963.7 mm at subtropical evergreen forest GT, and 21.8°C and 1493 mm at tropical evergreen forest XSBN). Soil types differ as well, with dark-brown earth at temperate mixed forest CB, yellow-red earth at subtropical evergreen forest GT and laterite earth at tropical evergreen forest XSBN. Additionally, the soil total P concentration also varies largely, with the lowest value (0.16 g kg^{-1}) at subtropical evergreen forest GT, followed by tropical evergreen forest XSBN (0.80 g kg^{-1}) and temperate mixed forest CB (1.67 g kg^{-1}; Supporting Information Table S1).

To ensure the comparability among different forest sites, only broad-leaved tree species were sampled for the consequent measurements of leaf reflectance spectra and multiple traits. Within the footprint of the crane towers, 77 trees from 9 dominant species at temperate mixed forest CB, 92 trees from 16 dominant species at subtropical evergreen forest GT and 88 trees from 33 dominant species at tropical evergreen forest XSBN were selected for subsequent measurements of leaf gas exchange, leaf reflectance spectra, leaf P fractions and other leaf morphological and biochemical traits (i.e. SLA, LWC, [Chl], [N], [P] and N : P) during the peak growing season (July–August) of 2023. Only sunlit mature leaves from the upper canopy were sampled for further measurements. The detailed protocols for these measurements are provided below, and the summary of the statistical characteristics of these measurements is presented in Tables S2–S5.

Field measurements

Leaf gas exchange Two branches, each 50–80 cm in length, were sampled from each tree before dawn and recut under water to avoid xylem embolism (Sperry, 2013; Wu *et al.*, 2019). From each branch, two sunlit mature leaves with similar growth status (i.e. similar coloration, size and rigidity) were then selected for gas exchange measurements. The excised branches were placed in individual buckets filled with water and kept in the shade. We used six portable Li-COR gas exchange systems (two LI-6400 XTs and four LI-6800s; Li-COR Inc., Lincoln, NE, USA) to measure the response of net assimilation rate (A) to intercellular CO_2 concentration (C_i) (commonly known as the A–C_i curve), following the protocols of Rogers *et al.* (2017) and Z.B. Yan *et al.* (2021), with details shown in Methods S1. Our previous study demonstrated that the results are not influenced by these two types of Li-COR gas exchange system (S.T. Liu *et al.*, 2023; Wu *et al.*, 2025). After measurements, we fitted A–C_i curves to a biochemical photosynthesis model (Farquhar *et al.*, 1980) using the code developed in MATLAB (Mathworks, Natick, MA, USA) by Wu *et al.* (2019) and Z.B. Yan *et al.* (2021). $V_{c,max}$, J_{max} and A_{sat} were then derived from these fitted A–C_i curves and standardized to a reference temperature of 25°C ($V_{c,max25}$, J_{max25} and A_{sat25}). $V_{c,max25}$ and J_{max25} were estimated using kinetic constants and temperature response functions as Bernacchi *et al.* (2013), while A_{sat} was standardized to A_{sat25} following Rowland *et al.* (2016). The three gas exchange parameters were transformed into the mass-based metrics with SLA for comparable analyses with the mass-based elemental concentrations.

Leaf reflectance spectra We measured leaf reflectance spectra immediately after conducting leaf gas exchange measurements with a portable handheld contact-type spectroradiometer (QualitySpec TREK; PANalytical, Boulder, USA; spectral full-range: 400–2500 nm; spectral resolution: ≤ 3 nm at 700 nm; ≤ 9.8 nm at 1400 nm; ≤ 8.1 nm at 2100 nm; sampling interval: linearly interpolated to 1 nm). Notably, the leaf reflectance spectra were measured on the same branches used for gas exchange measurements. During leaf reflectance spectra measurements, an internal quartz tungsten halogen bulb in the probe was used to illuminate the leaf samples upon a black background, with a 99% reflective Spectralon white panel (Labsphere Inc., North Dutton, NH, USA) serving as the reference standard (Wu *et al.*, 2019; Z.B. Yan *et al.*, 2021; S.W. Liu *et al.*, 2023). For each branch, we selected 6–10 mature and healthy leaves, measured the reflectance spectra at three to six positions on the adaxial side (avoiding the main veins) of each leaf and averaged the spectra to represent the spectral properties of the branch.

Leaf P fractions After leaf spectral measurements, we sampled mature leaves with similar growth status from the same branches used for gas exchange measurements. A portion of these leaves was used to assess the five fractions of leaf P (i.e. [P_i], [P_L], [P_N], [P_M] and [P_R]; in milligrams per gram). Leaf P fractions were sequentially extracted from freeze-dried leaves following the methodology adapted from Chapin & Kedrowski (1983) and Kedrowski (1983), with modifications as described by Hidaka & Kitayama (2011) and Yan *et al.* (2019). The data with greater than 90% recovery rates (i.e. the sum of the concentrations of leaf P fractions as a proportion of [P]) were accepted in this study. As a detailed description of P-fractionation analysis has been presented in Yan *et al.* (2019) and Tsujii *et al.* (2024), we briefly summarized the major steps of this approach in Methods S2.

Leaf biochemical and morphological traits The remaining sampled sunlit mature leaves with similar growth status were used to determine the six other morphological and biochemical traits, including SLA ($cm^2\ g^{-1}$), LWC ($g\ g^{-1}$), [Chl] ($mg\ g^{-1}$), [N] ($mg\ g^{-1}$), [P] ($mg\ g^{-1}$) and N : P ($g\ g^{-1}$). The details of measurements taken are shown in Methods S3. Then, PNUE and PPUE were calculated using A_{sat25} divided by [N] and [P], respectively.

Data analysis

In this study, we focused on exploring the variability in leaf P fractions using leaf traits and leaf reflectance spectra. A Shapiro–Wilk test was used to assess the normality of distributions for leaf P fractions and leaf traits across three forest sites. All the concentrations (i.e. [P_i], [P_L], [P_N], [P_R] and [P_M]) and proportions (i.e. rP_i, rP_L, rP_N, rP_R and rP_M) of leaf P fractions were deemed normal and untransformed in the subsequent analyses. The other leaf economic traits showed approximately log-normal distributions and were log_{10}-transformed. The data used for all analyses were based on individual tree level.

Variability in leaf P fractions and economic traits across forest types We used a one-way analysis of variance (ANOVA) with *post hoc* Tukey's HSD test to explore the changes in leaf P fractions and associated traits across forest types. Furthermore, to characterize the phylogenetic structure of leaf P fractions, we constructed a phylogenetic tree using the R package V.PHYLOMAKER (Jin & Qian, 2019) and then calculated the phylogenetic signal (i.e. Pagel's λ) using the *phylosignal* function from the R package PICANTE (Kembel *et al.*, 2010). Pagel's λ quantifies whether the distribution of a trait on a given phylogeny approximates that expected from a Brownian motion model of trait evolution ($\lambda = 1$) or is more labile than expected from such a model ($\lambda < 1$) (Pagel, 1999). A permutation test can be used to quantify whether the observed λ value deviates from that expected by a purely random (i.e. white noise) model of trait evolution. This test is performed by permuting trait values across the tips of the phylogeny 999 times to generate a null distribution. The rank of the observed λ in the null distribution can then be used to estimate a *P*-value (Swenson, 2014, 2019).

Relationships between leaf P fractions and economic traits To investigate the relationships between leaf P fractions and leaf traits, we conducted three analyses. First, a Pearson's correlation analysis, accompanied by heatmaps, was performed to evaluate correlations between leaf P fractions and leaf traits across forest types. Second, we used a principal component analysis (PCA) on leaf P fractions and leaf traits to explore multidimensional relationships among these traits across forest types. All traits were standardized by z-score method before PCA. The first two PCA axes were then delineated to visualize the trait space. Third, to explore the predictive power of easier-to-measure traits on leaf P fractions, we conducted multiple linear regressions as follows: lm (*Leaf P fractions* ~ *trait variables* + (1|*site*)) using the *lmer* function from the R package LME4 (Bates *et al.*, 2015). The variables included six easily measurable traits, including LWC, SLA, [Chl], [N], [P] and N : P. Models were selected based on the following criteria: (1) the model with the lowest Akaike information criterion value (Akaike, 1974); and (2) the variance inflation factor for each variable being less than 5 to avoid multicollinearity (Dobson, 2001; Hovenden *et al.*, 2019). Following these two criteria, we predicted the variability in leaf P fractions through the final optimal model below: lm (*Leaf P fractions* ~ *LWC* + *SLA* + *[Chl]* + *[N]*). To assess the performance of trait-based models, we calculated the average coefficient of determination (R^2) and the relative root means square error (%RMSE). Fourth, to partition the inter- and intraspecific variation of leaf P fractions within each site, we employed a general linear model based on ANOVA, following the method proposed by Guillén-Escribà *et al.* (2021). The model was specified as follows: lm (*Leaf P fractions* ~ *species*). Through this model, we partitioned the total variance into two components. The interspecific variance was represented by the percentage of variance explained by the 'species' term in the ANOVA-based general linear model, while the intraspecific variance was represented by the residuals.

Exploring the accuracy of spectral models in predicting leaf P fractions across forest types To assess the feasibility of leaf reflectance spectroscopy on predicting leaf P fractions, we developed spectral models and compared their performance with that of previously mentioned trait-based models. We integrated the partial least-squares regression (PLSR) method with the repeated double cross-validation (rdCV) method to develop cross-site spectral models of leaf P fractions using the Python library *scikit-learn* (Pedregosa *et al.*, 2011). The PLSR approach, which effectively handles high covariance among predictor variables and allows the number of explanatory variables to exceed the number of observations, has been widely used in spectral modeling of plant functional traits (Serbin *et al.*, 2019; Burnett *et al.*, 2021; Z.B. Yan *et al.*, 2021; Kothari *et al.*, 2023b). The rdCV method divided the whole dataset into calibration and independent validation subsets repeatedly using a cross-validation (outer CV loop), with the calibration subset further divided into training and testing components using a second cross-validation (inner CV loop; Filzmoser *et al.*, 2009). Specifically, 90% of the data were used as the calibration subset and 10% as the independent validation subset. Given that spectral model details have been

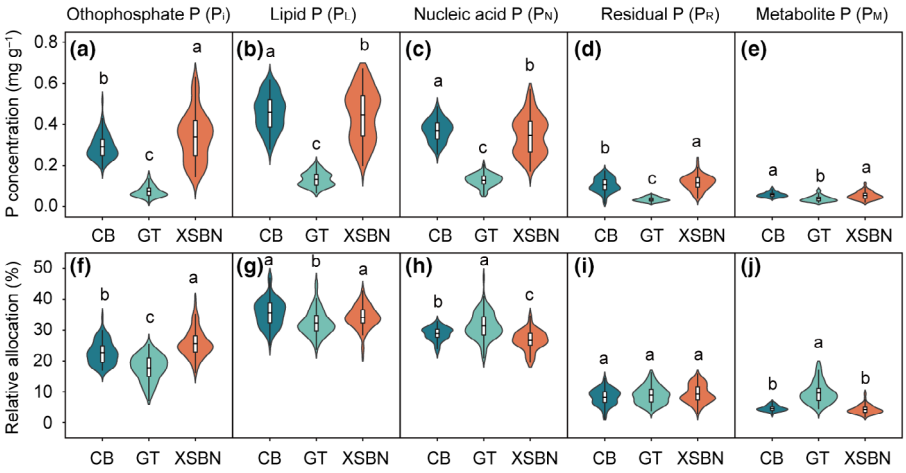

Fig. 2 Mass-based concentrations (a–e) and relative proportions (f–j) of leaf phosphorus (P) fractions across forest types. The central boxes within each violin plot show the interquartile range and median, and the whiskers extending 1.5 times the interquartile range or to the most extreme value. Significant differences among sites are shown as different lowercase letters for leaf P fractions based on one-way ANOVA with *post hoc* Tukey's HSD test. CB, Changbai Mountain; GT, Gutian Mountain; XSBN, Xishuangbanna.

elaborated in Dechant *et al.* (2017), Z.B. Yan *et al.* (2021) and Wu *et al.* (2025), we briefly summarized four main procedures in Methods S4. To assess the performance of spectral models, we calculated R^2 and %RMSE using the independent validation dataset for each of the 200 repetitions in the outer loop, thereby circumventing stochastic results disrupted by unrepresentative samples. To identify the significant spectral domains for predicting leaf P fractions, we calculated the mean Variable Importance in Projection (VIP) metrics across the 200 repetitions in the outer loop.

Results

Variability in leaf P fractions across diverse forest types

To address our first question regarding the variability in leaf P fractions, we cross-compared the mean and coefficient of variation (CV) of the concentrations and proportions of leaf P fractions across forest types, partitioned the total variance of leaf P fractions into intraspecific and interspecific components, and subsequently explored their phylogenetic structures. The concentrations of leaf P fractions were the lowest at the subtropical GT, which had the lowest soil P availability among the three studied sites (Fig. 2a–e; Table S1). Species at the tropical XSBN exhibited significantly higher [P_i] and [P_R] than [P_L] and [P_M], and significantly lower [P_N] than those at the temperate mixed forest CB (Fig. 2a–e). The concentrations of leaf P fractions from three forest sites exhibited remarkable variability, with [P_i] showing the highest CV (62%), followed by [P_R] (56%), [P_L] (52%), [P_N] (46%) and [P_M] (35%). The variability in the concentrations of leaf P fractions was mainly attributed to interspecific variance across three forest types (Fig. S1d). However, the relative contributions of intra- and interspecific variances diverged among forest types. Specifically, the temperate mixed forest CB and subtropical evergreen forest GT exhibited relatively higher intraspecific variance, whereas the tropical evergreen forest XSBN showed relatively higher interspecific variance (Fig. S1a–c). Moreover, the concentrations of these five P fractions demonstrated different phylogenetic signals across species from the three forest sites, with significant phylogenetic signals observed in [P_L] and [P_N], and no significant phylogenetic signals in [P_i], [P_R] and [P_M] (Fig. S2).

Regarding the proportions of P fractions, species at the subtropical evergreen forest GT with the lowest soil P availability had significantly higher rP_N and rP_M, and significantly lower rP_i and rP_L than at the temperate mixed forest CB and tropical evergreen forest XSBN (Fig. 2f–j). Compared with the temperate mixed forest CB, the tropical evergreen forest XSBN showed significantly higher rP_i, lower rP_N and comparable rP_L, rP_M and rP_R (Fig. 2f–j). Furthermore, the proportions of leaf P fractions across three forest sites exhibited remarkable variability, with rP_M showing the highest CV (54%), followed by rP_R (32%), rP_i (24%), rP_N (14%) and rP_L (13%). Interestingly, for each leaf P fraction, the variability in concentration was greater than that of proportion. The variability in the proportions of leaf P fractions was also primarily driven by interspecific variance across three forest types (Fig. S1h). Consistent with the concentrations of leaf P fraction, the proportions of leaf P fractions also exhibited higher intraspecific variance at the temperate mixed forest CB and subtropical evergreen forest GT, whereas the tropical evergreen forest XSBN displayed greater interspecific variance (Fig. S1e–g). In addition, compared with [P_M], rP_M exhibited a higher interspecific variance. Conversely, the interspecific variance of rPi, rP_L, rP_N and rP_R was lower than that of their concentrations (Fig. S1d,h). Additionally, the proportions of leaf P fractions exhibited no significant phylogenetic signals across species from the three forest sites (Fig. S1).

Relationships between leaf P fractions and economic traits across forest types

To explore the relationships between leaf P fractions and economics traits across forest types, we performed Pearson's correlation analysis and PCA. Initially, we found that plants at the subtropical GT, compared with the other two forests, exhibited conservative strategies, characterized by lower SLA, LWC, [Chl], nutrient concentrations and photosynthetic capacity (indicated by V_{cmax25}, J_{max25} and A_{sat25}), but higher N : P ratio and

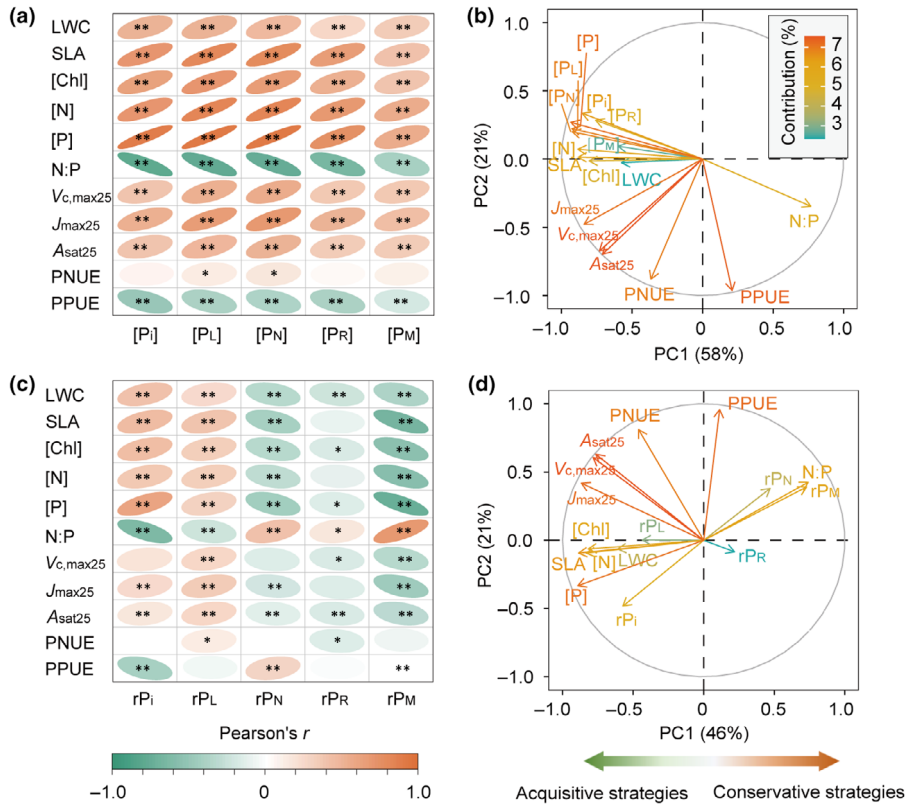

Fig. 3 Exploring cross-site relationships between leaf phosphorus (P) fractions and leaf traits using Pearson's correlation analyses (a, c) and principal component analysis (PCA) (b, d). Pearson's correlations among traits are presented in heat maps, with the intensity of color indicating the absolute value of Pearson's *r*. Significance is shown only if $P < 0.05$, with * indicating significance at $0.01 < P < 0.05$ and ** indicating significance at $P \leq 0.01$. The trait loadings on the right panels are delineated by principal component 1 (PC1) and principal component 2 (PC2), with the color gradient of the arrows indicating their contribution to the principal components. [Chl], leaf Chl concentration; [N], leaf N concentration; [P], leaf P concentration; [P_L], [P_M], [P_N], [P_R], [P_i], the concentrations of lipid P, metabolite P, nucleic acid P, residual P and orthophosphate P, respectively; A_{sat25}, light-saturated net photosynthetic rate standardized to 25°C; J_{max25}, the maximum electron transport rate standardized to 25°C; LWC, leaf water content; N, nitrogen; N : P, N to P ratio; PNUE, photosynthetic N-use efficiency; PPUE, photosynthetic P-use efficiency; rP_L, rP_M, rP_N, rP_R, rP_i, the relative proportions of lipid P, metabolite P, nucleic acid P, residual P and orthophosphate P per total leaf P concentration, respectively; SLA, specific leaf area; $V_{c,max25}$, the maximum carboxylation rate of the enzyme RuBisCO standardized to 25°C.

PPUE (Figs S3, S4). Furthermore, we found that the concentrations of leaf P fractions were positively associated with LWC, SLA, [Chl], [N], [P], V_{cmax25}, J_{max25} and A_{sat25}, but negatively correlated with N : P ratio and PPUE (Fig. 3a,b; Table S6). Regarding PCA, the first two principal components (PCs) accounted for 58% (PC1) and 21% (PC2) of the total variation in the concentrations of leaf P fractions and associated leaf traits (Fig. 3b). The PC1 axis predominantly represents a continuum from acquisitive to conservative strategy, associated with the decreasing LWC, SLA, [Chl], nutrient concentrations (i.e. [N], [P], [P_i], [P_L], [P_N], [P_M] and [P_R]) and photosynthetic capacity (indicated by V_{cmax25}, J_{max25} and A_{sat25}), and with increasing P limitation indicated by higher N : P ratio (Fig. 3b).

The relationships between the proportions of leaf P fractions and economic traits are more complex. Our results indicate that rP_M, rP_N and rP_R were negatively correlated with LWC, SLA, [Chl], nutrient concentrations and photosynthetic capacities, but positively correlated with N : P ratio (Fig. 3c,d; Table S7). By contrast, rP_L and rP_i showed opposite correlations with those leaf traits (Fig. 3c,d; Table S7). Photosynthetic P-use efficiency was significantly positively correlated with rP_N and rP_M, but significantly negatively correlated with rP_i (Fig. 3c,d; Table S7). Additionally, PCA indicated that the first two PCs accounted for 46% (PC1) and 21% (PC2) of the total variation in the proportions of leaf P fractions and associated leaf traits (Fig. 3d). Among these PCs, the PC1 axis predominately reflected the continuum from acquisitive to conservative strategy and the increasing P limitation and was negatively associated with rP_L and rP_i, but positively associated with rP_N and rP_M (Fig. 3d).

Prediction of leaf P fractions based on trait correlations and reflectance spectroscopy

Due to the challenges in measuring leaf P fractions, we further examined how to reliably estimate leaf P fractions using a trait-based approach and leaf reflectance spectroscopy. We cross-compared the performance of trait-based models with that of hyperspectral-based models. Our results demonstrate that the

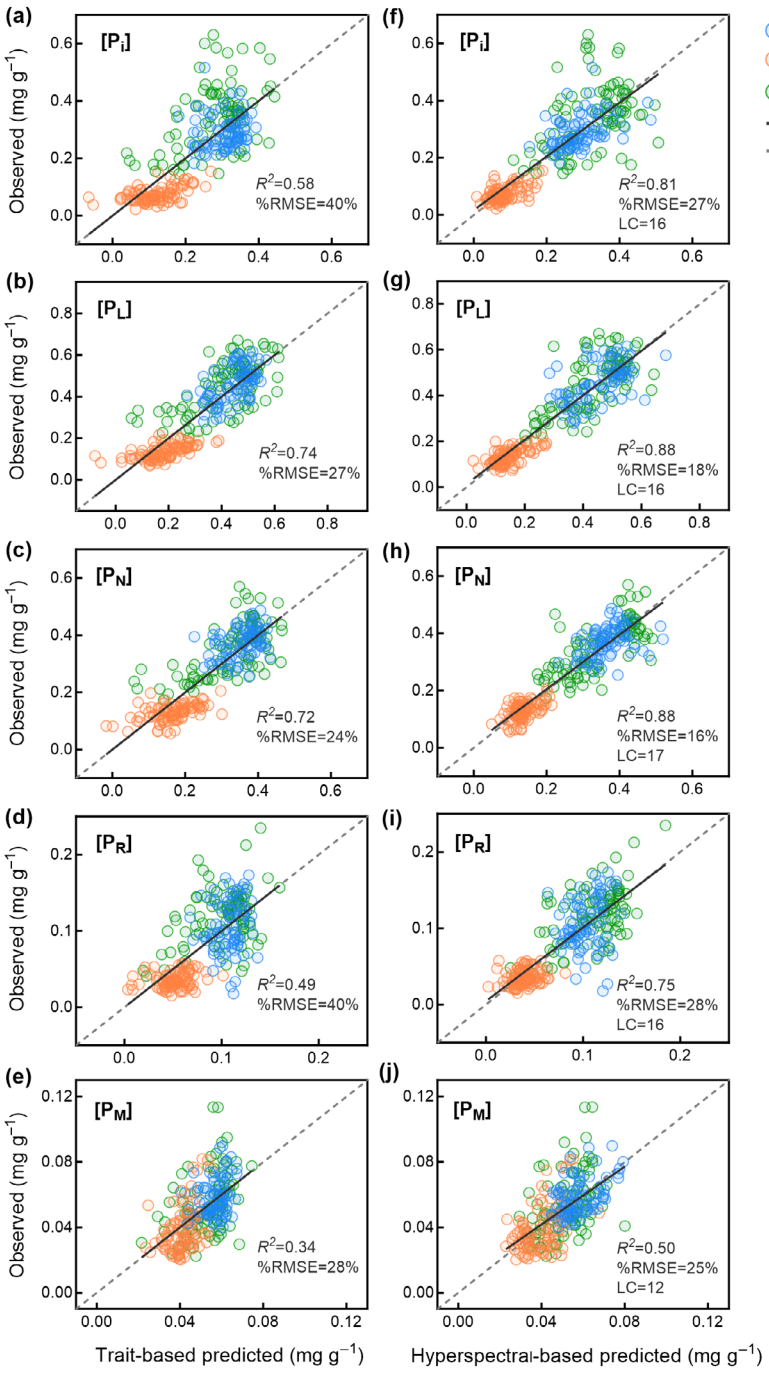

Fig. 4 Accuracy assessment for the predictions of mass-based concentrations of leaf phosphorus (P) fractions using leaf trait correlations and reflectance spectroscopy. The cross-site trait-based models of leaf P fractions (a–e) are performed by multiple linear regression, with explanatory variables as LWC (leaf water content), SLA (specific leaf area), [Chl] (leaf Chl concentration) and [N] (leaf N concentration). The cross-site spectral models of leaf P fractions (f–j) are performed by partial least-squares regression. The gray line represents the 1 : 1 line, and the black line indicates the ordinary least-squares regression fit. Three different-colored circles represent three forest types, with temperate mixed forest CB (Changbai Mountain) in blue, subtropical evergreen forest GT (Gutian Mountain) in orange and tropical evergreen forest XSBN (Xishuangbanna) in green. %RMSE, the relative root mean square of error; $[P_L]$, $[P_M]$, $[P_N]$, $[P_R]$, $[P_i]$, the concentrations of lipid P, metabolite P, nucleic acid P, residual P and orthophosphate P, respectively; LC, the optimal number of latent components; N, nitrogen; R^2, the adjusted coefficient of determination.

hyperspectral-based models outperformed the trait-based models in predicting the concentrations of leaf P fractions (R^2 = 0.50–0.88 vs 0.34–0.74, %RMSE = 16–28% vs 24–40%; Fig. 4). A similar pattern was observed when predicting the proportions of leaf P fractions, with hyperspectral models again showing superior performance: R^2 = 0.43–0.70 vs 0.06–0.45, %RMSE = 8–30% vs 12–40% (Fig. 5). Furthermore, both model types exhibited greater predictive power for the concentrations than for the proportions of leaf P fractions (Figs 4, 5). These findings verified that leaf reflectance spectroscopy provides a reliable and efficient alternative approach for estimating leaf P fractions, particularly for determining their concentrations.

To elucidate the intrinsic mechanisms underlying the spectral models of leaf P fractions, we used the VIP metrics from PLSR models to identify the significant spectral domains for predicting leaf P fractions (Fig. 6b,c). The overall trend in VIP variation in the concentrations and proportions of leaf P fractions resembles that of [P], demonstrating peaks in the visible range (VIR, 400–700 nm) and near-infrared range

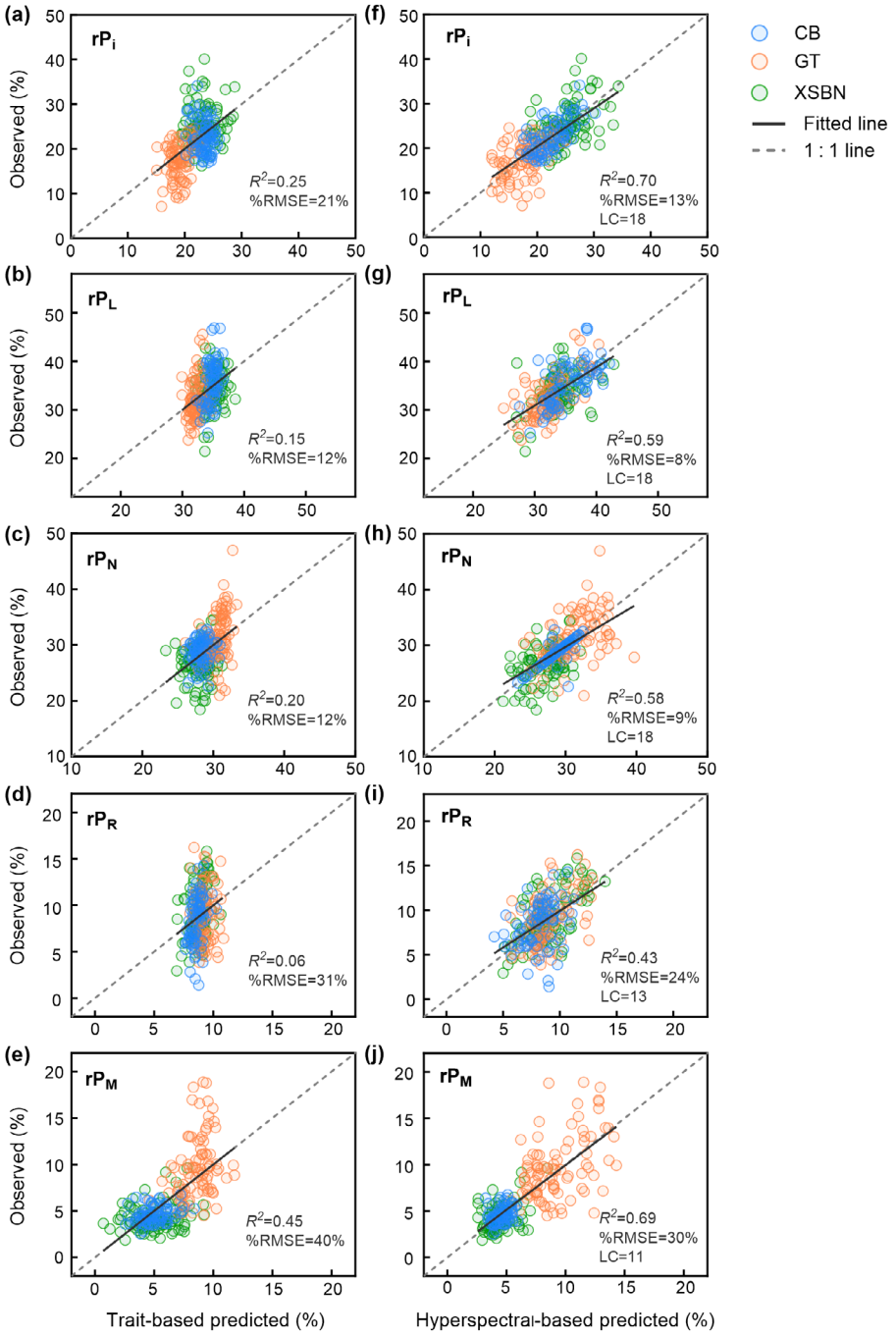

Fig. 5 Accuracy assessment for the predictions of the relative proportions of leaf phosphorus (P) fractions using leaf trait correlations and reflectance spectroscopy. The cross-site trait-based models of leaf P fractions (a–e) are performed by multiple linear regression, with explanatory variables as LWC (leaf water content), SLA (specific leaf area), [Chl] (leaf Chl concentration) and [N] (leaf N concentration). The cross-site spectral models of leaf P fractions (f–j) are performed by partial least-squares regression. The gray line represents the 1 : 1 line, and the black line indicates the ordinary least-squares regression fit. Three different-colored circles represent three forest types, with temperate mixed forest CB (Changbai Mountain) in blue, subtropical evergreen forest GT (Gutian Mountain) in orange and tropical evergreen forest XSBN (Xishuangbanna) in green. %RMSE, the relative root mean square of error; LC, the optimal number of latent components; N, nitrogen; rP_L, rP_M, rP_N, rP_R, rP_i, the relative proportions of lipid P, metabolite P, nucleic acid P, residual P and orthophosphate P per total leaf P concentration, respectively; R^2, the adjusted coefficient of determination.

(NIR, 700–1300 nm), accompanied by a trough in the shortwave infrared range (SWIR, 1300–2500 nm; Fig. 6). Specifically, our cross-site spectral models for leaf P fractions identified the important bands as follows (VIP > 1; S.W. Liu *et al.*, 2023): (1) 400–480 nm and 510–650 nm in the VIR; (2) 700–800 nm in the red edge band; (3) 800–900 nm in the NIR; and (4) 1300–1900 nm and 2000–2300 nm in the SWIR (Fig. 6b,c). Additionally, we found that the VIP spectra of P_M in the VIR were distinctly separated from those of the other four P fractions, regardless of their concentrations or proportions (Fig. 6b,c).

Discussion

Allocation of leaf P among different fractions provides insights into P-use strategies and potential mechanisms in response to changing environments (Yan *et al.*, 2019; L. Yan *et al.*, 2021; Hawkesford *et al.*, 2022; Lambers, 2022; Meng *et al.*, 2025). However, there is no coherent understanding and efficient monitoring of fine-scale variability in leaf P fractions across forest types. Here, we revealed the variability in leaf P fractions associated with leaf economic traits and reflectance spectra across forest types and achieved three key findings. First, we found that in

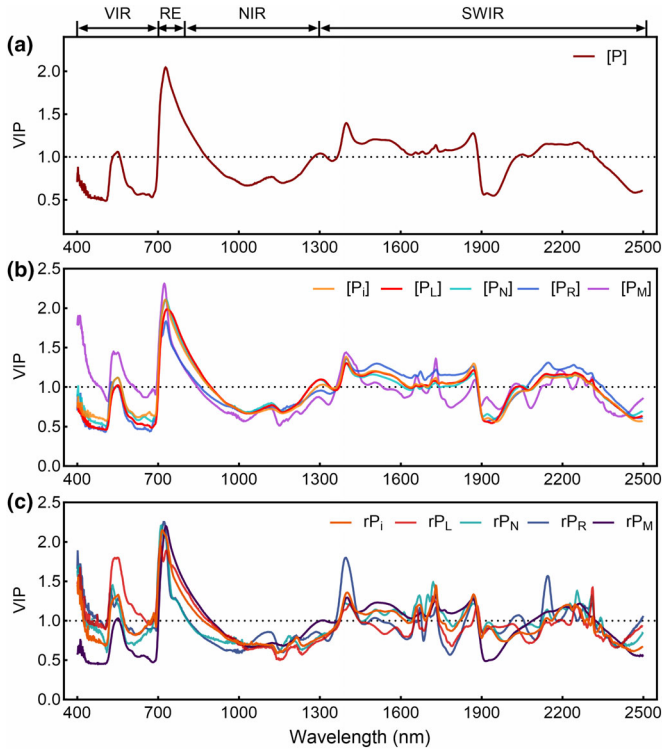

Fig. 6 Assessing the reflectance contributions to the cross-site spectral models of leaf phosphorus (P) concentration ([P]) and leaf P fractions using the partial least-squares regression (PLSR) approach. The variable importance in projection (VIP) spectrum of the PLSR models was used to identify the sensitive spectral domains for the spectral models of [P] (a), the concentrations of leaf P fractions (b), and the relative proportions of leaf P fractions (c). The black dashed line represents VIP of 1 (Wold *et al*., 2001; S. W. Liu *et al*., 2023), which was denoted as the threshold to identify the important spectral regions responsible for the spectral modeling. [P_L], [P_M], [P_N], [P_R], [P_i], the concentrations of lipid P, metabolite P, nucleic acid P, residual P and orthophosphate P, respectively; N, nitrogen; NIR, near-infrared range (800–1300 nm); RE, red edge range (700–800 nm); rP_L, rP_M, rP_N, rP_R, rP_i, the relative proportions of lipid P, metabolite P, nucleic acid P, residual P and orthophosphate P per total leaf P concentration, respectively; SWIR, shortwave infrared range (1300–2500 nm); VIR, visible range (400–700 nm).

forests with lower soil P availability, plants have lower concentrations of all five leaf P fractions, lower rP_i and rP_L, but higher rP_N and rP_M, demonstrating a trade-off among leaf P fractions for increasing PPUE under P-limited conditions (Figs 2, 3c,d; Tables S1, S7). Second, we revealed that the concentrations and proportions of leaf P fractions varied along the LES, representing a continuum from acquisitive to conservative trait syndromes, together with decreasing concentrations of leaf P fractions, rP_i and rP_L but increasing rP_N and rP_M (Fig. 3b,d). This pattern underscores the link between leaf P allocation and plant functional strategies. Third, we demonstrated that leaf reflectance spectroscopy outperformed leaf trait correlations in predicting both the concentrations and proportions of leaf P fractions across forest types (Figs 4, 5). Taken together, our study expands our mechanistic understanding of the variability in leaf P fractions and highlights the substantial potential of leaf reflectance spectroscopy for efficient and high-throughput monitoring of plant P-use strategies and P cycling across diverse ecosystems.

Variability in leaf P fractions across diverse forest types

Our results revealed substantial variation in the concentrations of leaf P fractions within and across forest types, which span large environmental gradients. Generally, the mean concentrations of leaf P fractions across forest types were the highest in P_L, followed by P_N, P_i, P_R and P_M (Fig. 2a–e). Consistent with previous studies, we found that P_i exhibited the greatest variation among the concentrations of leaf P fractions, likely due to its buffering role (Veneklaas *et al*., 2012; Yan *et al*., 2019; Suriyagoda *et al*., 2022). Furthermore, plants at the subtropical GT, with the lowest soil P availability among three sites, had the lowest concentrations of leaf P fractions (Fig. 2a–e; Table S1), suggesting that increasing P limitation reduces the concentrations of leaf P fractions (Hayes *et al*., 2014; Yan *et al*., 2019), as supported by the negative correlations between the concentrations of leaf P fractions and the N : P ratio (Fig. 3a,b; Table S6). This pattern of leaf P fractions across forest types aligns with several previous field-based studies conducted in Mediterranean shrublands, sclerophyll forests and temperate evergreen forests in Australia (Yan *et al*., 2019; Tsujii *et al*., 2023, 2024; Liang *et al*., 2024), as well as tropical montane rain forests in Malaysian Borneo (Hidaka & Kitayama, 2011, 2013; Tsujii *et al*., 2017). It is primarily attributed to the consumption of P_i stored in vacuoles, low levels of phospholipids, slow protein turnover and weak metabolic activity in low-P soils (White & Hammond, 2008; Veneklaas *et al*., 2012; Lambers, 2022).

We also observed substantial variation in the proportions of leaf P fractions within and across three forest types. Plants at the subtropical GT, with the relatively lower soil P availability, had lower rP_i and rP_L but higher rP_N and rP_M (Fig. 2f–j; Table S1). This finding suggests that under conditions of increasing P limitation, plants reduce their storage of P_i and investment in the membrane system, while allocating more P to P_N and P_M, which are critical for the photosynthetic apparatus, thus maintaining high PPUE (Ostertag, 2010; Veneklaas *et al*., 2012; Lagace & Ridgway, 2013; Yan *et al*., 2019). The correlations between the proportions of leaf P fractions, N : P ratio and PPUE observed in our study further support this finding (Fig. 3c,d; Table S7). Besides, this finding is partly supported by previous work reported in tropical montane rain forest, which also found that plants reduce rP_L to maintain high PPUE in low-P soils (Hidaka & Kitayama, 2013). However, conflicting results have been reported in some studies regarding changes in the proportions of leaf P fractions under divergent soil P conditions with relatively constant or species-specific allocation patterns across habitats and seasons, primarily due to limited study sites and species (Hidaka & Kitayama, 2011, 2013; Yan *et al*., 2019; S.T. Liu *et al*., 2023; Tsujii *et al*., 2023, 2024). Therefore, larger datasets encompassing more species and broader environmental gradients are needed to better explore the pattern of leaf P fractions and, ultimately, P-use strategies.

Leaf trait-based understanding and prediction of leaf P fractions

Exploring associations between leaf traits and P fractions enhances our mechanistic understanding of how plants allocate leaf P to adapt to varying environmental conditions (Yan *et al.*, 2019; L. Yan *et al.*, 2021; Lambers, 2022; Tsujii *et al.*, 2023, 2024). Our results indicated that leaf P fractions varied along the LES, representing a continuum from the acquisitive to conservative trait syndrome, characterized by decreases in the light-capturing surfaces (indicated by SLA), LWC, investment in carbon assimilation (indicative of [Chl], [N] and [P]) and photosynthetic capacity (indicated by $V_{c,max25}$, J_{max25} and A_{sat25}), but increases in N : P ratio and PPUE (Fig. 3; Tables S6, S7). Specifically, our findings highlighted that, as plants shift from the acquisitive to conservative strategy, the concentrations of leaf P fractions, rP_i and rP_L, decreased, while rP_N and rP_M increased, particularly under P-limited conditions (Fig. 3d). This finding suggests that under nutrient-deficient conditions, plants exhibiting conservative strategies allocate more leaf P to P_N and P_M, while reducing allocation to P_i and P_L. This shift can be attributed to the necessity for plants to invest more P in the turnover of core photosynthetic proteins and metabolites, thereby supporting high PPUE (Veneklaas *et al.*, 2012; Suriyagoda *et al.*, 2022). Meanwhile, the functions of P_i and P_L can be partially compensated by other substances, allowing for P reallocation toward photosynthesis (Lambers *et al.*, 2012; Poirier *et al.*, 2022). For instance, during periods of P starvation, enzymes that depend on P_i may be substituted by those that depend on inorganic pyrophosphate (Poirier *et al.*, 2022), and P-rich phospholipids can be replaced by P-free lipids, such as galactolipids (Lambers *et al.*, 2012). Considering a more extensive species number, diverse ecosystem types and multi-traits, our trait-based interpretation of leaf P-allocation strategies is likely more representative, general and robust than previous studies with a relatively narrow breadth of species diversity, environmental gradients and trait dimensions (Hidaka & Kitayama, 2011, 2013; Mo *et al.*, 2019; Yan *et al.*, 2019; L. Yan *et al.*, 2021; Tsujii *et al.*, 2023, 2024).

Furthermore, the empirical relationships between leaf traits and P fractions provide insights into the formulation of empirical equations to derive the difficult-to-measure leaf P fractions from those easier-to-measure traits (Hidaka & Kitayama, 2011, 2013; Tsujii *et al.*, 2023, 2024). Our results indicate that the four easily measurable leaf traits (i.e. LWC, SLA, [Chl] and [N]) could indirectly infer the concentrations of leaf P fractions across various scales, from individual trees to contrasting forest types (R^2 = 0.34–0.74; Fig. 4a–e). The capacity of these traits in predicting the concentrations of leaf P fractions was much greater than that of those with each single trait, as observed in our study (R^2 = 0.08–0.69; Fig. 3a, Table S6), and in previous studies (R^2 = 0.01–0.66) (Hidaka & Kitayama, 2011, 2013; Zhang *et al.*, 2018; Tsujii *et al.*, 2023, 2024), suggesting that the variability in leaf P fractions is associated with multidimensional traits. Nevertheless, these traits were much less effective at predicting the proportions compared with the concentrations of leaf P fractions (R^2 = 0.06–0.45 vs 0.34–0.74; Fig. 4), likely due to the relatively conservative nature of the proportions across species and forest types (CV = 13–54% vs 35–62%). Collectively, our results imply that, to some extent, leaf P fractions can be estimated from those relatively easier-to-measure traits with extensive spatial coverage (Wright *et al.*, 2005; Reich *et al.*, 2007; Berzaghi *et al.*, 2020). However, the generalizability of the trait-based approach still requires larger datasets encompassing more species and broader environmental gradients for further validation.

Moreover, while the four traits (i.e. LWC, SLA, [Chl] and [N]) jointly explain part of the variability in cross-site leaf P fractions, there still remains a substantial amount of unexplained variance, particularly in $[P_M]$, rP_L, rPN and rP_R (Figs 4, 5). This uncertainty may be linked to many other unconsidered factors, such as microclimate and soil properties (Yan *et al.*, 2019), evolutionary history (Yan *et al.*, 2023; Schweiger & Schweiger, 2024), hydraulic traits (e.g. water potential; S.T. Liu *et al.*, 2023; Castillo-Argaez *et al.*, 2024) and finer photosynthetic traits (e.g. light energy utilization in PSII, redox state of PSI and cyclic electron flow; L. Yan *et al.*, 2021). The current lack of direct quantitative evidence supporting these potential relationships warrants further research to elucidate the mechanisms underpinning the variability in leaf P fractions across forest types by integrating more relevant abiotic and biotic factors.

Spectroscopy provides a promising alternative for monitoring and understanding the cross-site variability in leaf P fractions

To our knowledge, this is the first study to leverage leaf reflectance spectroscopy to elucidate the variability in leaf P fractions across forest types, although previous studies have highlighted the substantial potential of leaf reflectance spectroscopy in predicting [P] across forest types (Fig. S5; Asner *et al.*, 2014; Kothari *et al.*, 2023a, 2023b; S.W. Liu *et al.*, 2023; Wijewardane *et al.*, 2023). We observed that the spectroscopy-based predictive capacity for the proportions of leaf P fractions is lower than that for the concentrations of leaf P fractions (Fig. 5), possibly due to the stability of these proportions across species and forest types (Figs 2, S1). Furthermore, the predictive accuracy of spectral models varied among these five P fractions, which is higher for $[P_i]$, $[P_L]$, $[P_N]$ and $[P_R]$ than for $[P_M]$, and higher for rP_i and rP_M than for rP_L, rP_N and rP_R (Figs 4, 5). This result may be attributed to the narrow range of leaf traits across forest types in the training dataset, which restricts the development of more accurate and generalized spectral-trait models (Wu *et al.*, 2019; Z.B. Yan *et al.*, 2021; Kothari *et al.*, 2023a). Nonetheless, our findings verify that leaf reflectance spectroscopy is a promising alternative for filling observational gaps in leaf P fractions. Particularly, our study highlights that leaf reflectance spectroscopy can decipher not only the fine-scale leaf P nutrient status indicated by the concentrations of leaf P fractions but also the leaf P-allocation strategies indicated by the proportions of leaf P fractions (Mo *et al.*, 2019; Yan *et al.*, 2019; Lambers, 2022; Tsujii *et al.*, 2024).

Interestingly, our results highlighted that leaf reflectance spectroscopy outperformed traditional leaf trait correlations in

predicting the cross-site variability in leaf P fractions in terms of both the concentrations (R^2 = 0.50–0.88 vs 0.34–0.74, %RMSE = 16–28% vs 24–40%) and the relative proportions (R^2 = 0.43–0.70 vs 0.06–0.45, %RMSE = 8–30% vs 12–40%; Figs 4, 5). The significant spectral domains for predicting leaf P fractions, indicated by VIP, may explain the better predictive capacity of spectral models. Given the lack of distinct spectral absorption features for P chemical bonds, spectral models of leaf P fractions likely depend on features linked to covarying traits that shape spectral changes, rather than the target traits ('constellation effects'; Chadwick & Asner, 2016; Nunes *et al.*, 2017). The sensitive spectral domains of four variables in trait-based models (i.e. LWC, SLA, [Chl] and [N]; concentrating on 500–800 nm) partially overlap with those of leaf P fractions (400–480 nm, 510–650 nm, 700–800 nm, 800–900 nm, 1300–1900 nm and 2000–2300 nm; Fig. 6b,c; Ely *et al.*, 2019; Z.B. Yan *et al.*, 2021; Kothari *et al.*, 2023a; Wu *et al.*, 2025), explaining why trait-based models capture limited variation of leaf P fractions. The spectral domains of leaf P fractions also capture signals from other P-associated but unmeasured traits, such as water (1450, 1650, 1940 and 2200 nm), proteins (1980, 2130 and 2240 nm), lignin (1420 nm), sugars (2320 nm), starch (1900 nm) and oils (2310 nm) (Curran, 1989; Ely *et al.*, 2019; Féret *et al.*, 2021; N.F. Liu *et al.*, 2023). This likely accounts for the superior predictive accuracy of spectroscopy-based models compared with that of trait-based models.

Moreover, we found that the VIP spectra of P_M in the VIR were distinctly separated from the other four P fractions, regardless of their concentrations or proportions (Figs 6b,c, S6). The high VIP of [P_M] in the VIR may be attributed to the tight and direct association between P_M and the light-dependent reaction. The key metabolic P compounds, such as $NADP^+$, NADPH, ATP and ADP directly participate in the light reaction. Yan *et al.* (2019) observed that a higher level of P_M is associated with lower photoinhibition and greater photochemical efficiency. This indicates that an adequate supply of P_M is essential for the light-harvesting and energy-conversion processes. The optical properties of leaves in the VIR are dominated by the strong absorption of solar energy by photosynthetic pigments (Ustin *et al.*, 2009). Interestingly, the absorption peaks of these pigments, as well as the structures of Photosystem I and Photosystem II, where the light reactions occur, correspond to the peaks in the VIP spectrum of [P_M] (Croce & van Amerongen, 2020). This means that the spectral information in the VIR is highly related to the photosynthetic processes in which P_M is deeply involved. However, direct evidence differentiating the spectral bands between rP_M and the relative proportions of the other four P fractions remains lacking, warranting further studies to elucidate the underlying mechanisms that produce the observed spectral responses. Overall, our findings suggest that other unmeasured traits or states may also participate in the prediction of leaf P fractions in the leaf reflectance spectra, further highlighting why the spectroscopy-based method outperformed the trait-based method for predicting leaf P fractions in our study.

Implications and future directions

Our findings enhance our understanding of leaf P-use strategies and plant P cycle processes across diverse forest ecosystems. While most previous studies have focused on the site- or species-specific variability in leaf P fractions in a climate zone (Hidaka & Kitayama, 2011; Yan *et al.*, 2019; S.T. Liu *et al.*, 2023; Tsujii *et al.*, 2023, 2024), our study deepens the understanding of plant P-use strategies by linking leaf P fractions to multidimensional leaf economic traits across different climate zones. This study emphasizes that leaf P-allocation strategies are governed by adaptive strategies represented within the LES, illustrating a continuum from acquisitive to conservative trait syndromes (Reich *et al.*, 1997; Wright *et al.*, 2004). Furthermore, we demonstrate the substantial potential of leaf reflectance spectroscopy as a promising alternative for characterizing the variability in leaf P fractions, directly addressing current spatial coverage gaps.

To deepen our understanding of leaf P-use strategies, we identify two critical next steps. First, additional efforts are urgently needed to capture a wider range of leaf traits and spectral variations across representative biomes, considering vertical structural gradients and the entire growing season (Serbin *et al.*, 2014; Chlus *et al.*, 2020; Davidson *et al.*, 2023; Lamour *et al.*, 2023; Ji *et al.*, 2024). This will enable us to decipher the relative contributions of long-term evolutionary history and current environmental conditions to the observed variations in leaf P fractions (Figs 1, S2; Yan *et al.*, 2023; Schweiger & Schweiger, 2024). Second, leaf-scale spectral modeling of leaf P fractions requires expansions from leaf to ecosystem scales through imaging spectrometers on various platforms, including unoccupied aerial systems, piloted airborne sensors and spaceborne satellites (Serbin & Townsend, 2020; Wang *et al.*, 2020; S.W. Liu *et al.*, 2023). Then, we can elucidate intricate scale-dependent mechanisms, monitor leaf P fractions, plant P-use strategies and refine our understanding of biogeochemical cycling across large spatial scales (Serbin & Townsend, 2020; S.W. Liu *et al.*, 2023). Overall, our findings not only advance the understanding of plant P-use strategies but also inform efforts to improve physiological representations of P cycle processes in land surface models, thereby enhancing predictions of ecosystem productivity and terrestrial carbon stocks (Rogers *et al.*, 2017; Jiang *et al.*, 2019, 2024). Emphasizing these critical pathways will be vital for better managing forest health and biodiversity in the context of a changing climate.

Acknowledgements

This work was supported by the National Natural Science Foundation of China (nos.: 32471573 and 32401379) and Key Talent Project of the State Key Laboratory of Vegetation and Environmental Change (LVEC-2023rc01). JW was supported by the National Natural Science Foundation of China (no.: 31922090), the HKU Seed Funding for Strategic Interdisciplinary Research Scheme, Hong Kong Research Grant Council Collaborative Research Fund (no.: C5062-21GF) and the Innovation and

Technology Fund (funding support to State Key Laboratory of Agrobiotechnology). SPS is supported by the NASA Surface Biology and Geology Mission. PBR was supported by the National Science Foundation ASCEND Biology Integration Institute (NSF-DBI-2021898). MJ acknowledges the funding support from the Zhejiang Provincial Natural Science Foundation of China (LZ23C030001 and LR24C030001). NG Smith acknowledges support from the Directorate for Biological Sciences of the US National Science Foundation (DEB-2045968). NG Swenson was supported by the Directorate for Biological Sciences of the US National Science Foundation (DEB-2124466). JP and JS were supported by the Spanish Government grants PID2022-140808 NB-I00 and TED2021-132627 B–I00 funded by MCIN, AEI/10.13039/ 501100011033 European Union Next Generation EU/PRTR. We extend our gratitude to the Research Station of Changbai Mountain Forest Ecosystems, the Zhejiang Qianjiangyuan Forest Biodiversity National Observation and Research Station and the National Forest Ecosystem Research Station at Xishuangbanna for providing the experimental platform.

Competing interests

None declared.

Author contributions

ZY and TD conceived and designed this research. TD, FW, NY, WX, GD and JD carried out the experiments and fieldwork. TD performed the data processing and analyses and drafted the initial manuscript with valuable input from ZY. TD, FW, YT, PAT, NY, WX, SL, NG Swenson, JL, WH, NG Smith, YS, LY, DT, MJ, ZW, XL, GD, JD, JS, PBE, HL, SPS, JP, JW and ZY reviewed and contributed to the final manuscript.

ORCID

Tingting Dong https://orcid.org/0009-0006-2987-1645
Wenxuan Han https://orcid.org/0000-0001-8678-7147
Mingkai Jiang https://orcid.org/0000-0002-9982-9518
Hans Lambers https://orcid.org/0000-0002-4118-2272
Julien Lamour https://orcid.org/0000-0002-4410-507X
Shuwen Liu https://orcid.org/0009-0004-0916-2257
Xiaojuan Liu https://orcid.org/0000-0002-9292-4432
Josep Peñuelas https://orcid.org/0000-0002-7215-0150
Peter B. Reich https://orcid.org/0000-0003-4424-662X
Jordi Sardans https://orcid.org/0000-0003-2478-0219
Shawn P. Serbin https://orcid.org/0000-0003-4136-8971
Yue Shi https://orcid.org/0009-0000-8531-9480
Nicholas G. Smith https://orcid.org/0000-0001-7048-4387
Nathan G. Swenson https://orcid.org/0000-0003-3819-9767
Di Tian https://orcid.org/0000-0002-0389-8683
Philip A. Townsend https://orcid.org/0000-0001-7003-8774
Yuki Tsujii https://orcid.org/0000-0003-3646-8142
Zhihui Wang https://orcid.org/0000-0003-1064-7820
Fengqi Wu https://orcid.org/0000-0002-6512-6830
Jin Wu https://orcid.org/0000-0001-8991-3970
Li Yan https://orcid.org/0000-0003-3937-2509
Zhengbing Yan https://orcid.org/0000-0002-5028-8167

Data availability

The data and code that support the findings of this study are available from the figshare dataset using the following link: https://doi.org/10.6084/m9.figshare.28675304.

References

Akaike H. 1974. A new look at the statistical model identification. *IEEE Transactions on Automatic Control* **19**: 716–723.

Asner GP, Martin RE, Carranza-Jiménez L, Sinca F, Tupayachi R, Anderson CB, Martinez P. 2014. Functional and biological diversity of foliar spectra in tree canopies throughout the Andes to Amazon region. *New Phytologist* **204**: 127–139.

Bates D, Mächler M, Bolker BM, Walker SC. 2015. Fitting Linear Mixed-Effects Models Using *lme4*. *Journal of Statistical Software* **67**: 1–48.

Bernacchi CJ, Bagley JE, Serbin SP, Ruiz-Vera UM, Rosenthal DM, Van Loocke A. 2013. Modelling C_3 photosynthesis from the chloroplast to the ecosystem. *Plant, Cell & Environment* **36**: 1641–1657.

Berzaghi F, Wright IJ, Kramer K, Oddou-Muratorio S, Bohn FJ, Reyer CPO, Sabaté S, Sanders TGM, Hartig F. 2020. Towards a new generation of trait-flexible vegetation models. *Trends in Ecology & Evolution* **35**: 191–205.

Bieleski RL. 1968. Effect of phosphorus deficiency on levels of phosphorus compounds in Spirodela. *Plant Physiology* **43**: 1309–1316.

Burnett AC, Anderson J, Davidson KJ, Ely KS, Lamour J, Li Q, Morrison BD, Yang D, Rogers A, Serbin SP. 2021. A best-practice guide to predicting plant traits from leaf-level hyperspectral data using partial least squares regression. *Journal of Experimental Botany* **72**: 6175–6189.

Castillo-Argaez R, Sapes G, Mallen N, Lippert A, John GP, Zare A, Hammond WM. 2024. Spectral ecophysiology: hyperspectral pressure-volume curves to estimate leaf turgor loss. *New Phytologist* **242**: 935–946.

Chadwick KD, Asner GP. 2016. Tropical soil nutrient distributions determined by biotic and hillslope processes. *Biogeochemistry* **127**: 273–289.

Chapin FS, Kedrowski RA. 1983. Seasonal changes in nitrogen and phosphorus fractions and autumn retranslocation in evergreen and deciduous taiga trees. *Ecology* **64**: 376–391.

Chen LT, Zhang Y, Nunes MH, Stoddart J, Khoury S, Chan AHY, Coomes DA. 2022. Predicting leaf traits of temperate broadleaf deciduous trees from hyperspectral reflectance: can a general model be applied across a growing season? *Remote Sensing of Environment* **269**: 112767.

Chlus A, Kruger EL, Townsend PA. 2020. Mapping three-dimensional variation in leaf mass per area with imaging spectroscopy and lidar in a temperate broadleaf forest. *Remote Sensing of Environment* **250**: 112043.

Croce R, van Amerongen H. 2020. Light harvesting in oxygenic photosynthesis: structural biology meets spectroscopy. *Science* **369**: eaay933.

Croft H, Chen JM, Luo XZ, Bartlett P, Chen B, Staebler RM. 2017. Leaf chlorophyll content as a proxy for leaf photosynthetic capacity. *Global Change Biology* **23**: 3513–3524.

Curran PJ. 1989. Remote sensing of foliar chemistry. *Remote Sensing of Environment* **30**: 271–278.

Davidson KJ, Lamour J, McPherran A, Rogers A, Serbin SP. 2023. Seasonal trends in leaf-level photosynthetic capacity and water use efficiency in a North American Eastern deciduous forest and their impact on canopy-scale gas exchange. *New Phytologist* **240**: 138–156.

Dechant B, Cuntz M, Vohland M, Schulz E, Doktor D. 2017. Estimation of photosynthesis traits from leaf reflectance spectra: correlation to nitrogen content as the dominant mechanism. *Remote Sensing of Environment* **196**: 279–292.

Dobson AJ. 2001. Model selection. In: Dobson AJ, ed. *An introduction to generalized linear models*. New York, NY, USA: Chapman and Hall/CRC, 91–92.

Du EZ, Terrer C, Pellegrini AFA, Ahlström A, van Lissa CJ, Zhao X, Xia N, Wu XH, Jackson RB. 2020. Global patterns of terrestrial nitrogen and phosphorus limitation. *Nature Geoscience* **13**: 221–226.

Elser JJ, Bracken MES, Cleland EE, Gruner DS, Harpole WS, Hillebrand H, Ngai JT, Seabloom EW, Shurin JB, Smith JE. 2007. Global analysis of nitrogen and phosphorus limitation of primary producers in freshwater, marine and terrestrial ecosystems. *Ecology Letters* **10**: 1135–1142.

Elvidge CD. 1990. Visible and near infrared reflectance characteristics of dry plant materials. *International Journal of Remote Sensing* **11**: 1775–1795.

Ely KS, Burnett AC, Lieberman-Cribbin W, Serbin SP, Rogers A. 2019. Spectroscopy can predict key leaf traits associated with source-sink balance and carbon-nitrogen status. *Journal of Experimental Botany* **70**: 1789–1799.

Farquhar GD, Caemmerer SV, Berry JA. 1980. A biochemical model of photosynthetic CO_2 assimilation in leaves of C_3 species. *Planta* **149**: 78–90.

Féret JB, Berger K, de Boissieu F, Malenovský Z. 2021. PROSPECT-PRO for estimating content of nitrogen-containing leaf proteins and other carbon-based constituents. *Remote Sensing of Environment* **252**: 112173.

Féret JB, Gitelson AA, Noble SD, Jacquemoud S. 2017. PROSPECT-D: towards modeling leaf optical properties through a complete lifecycle. *Remote Sensing of Environment* **193**: 204–215.

Féret JB, le Maire G, Jay S, Berveiller D, Bendoula R, Hmimina G, Cheraiet A, Oliveira JC, Ponzoni FJ, Solanki T *et al.* 2019. Estimating leaf mass per area and equivalent water thickness based on leaf optical properties: potential and limitations of physical modeling and machine learning. *Remote Sensing of Environment* **231**: 110959.

Filzmoser P, Liebmann B, Varmuza K. 2009. Repeated double cross validation. *Journal of Chemometrics* **23**: 160–171.

Gill AK, Gaur S, Sneller C, Drewry DT. 2024. Utilizing VSWIR spectroscopy for macronutrient and micronutrient profiling in winter wheat. *Frontiers in Plant Science* **15**: 1426077.

Guillén-Escribà C, Schneider FD, Schmid B, Tedder A, Morsdorf F, Furrer R, Hueni A, Niklaus PA, Schaepman ME. 2021. Remotely sensed between individual functional trait variation in a temperate forest. *Ecology and Evolution* **11**: 10834–10867.

Hawkesford MJ, Cakmak I, Coskun D, De Kok LJ, Lambers H, Schjoerring JK, White PJ. 2022. Functions of macronutrients. In: Rengel Z, Cakmak I, White PJ, eds. *Marschner's mineral nutrition of plants*. London, US: Elsevier, 201–281.

Hayes P, Turner BL, Lambers H, Laliberté E. 2014. Foliar nutrient concentrations and resorption efficiency in plants of contrasting nutrient-acquisition strategies along a 2-million-year dune chronosequence. *Journal of Ecology* **102**: 396–410.

Hidaka A, Kitayama K. 2011. Allocation of foliar phosphorus fractions and leaf traits of tropical tree species in response to decreased soil phosphorus availability on Mount Kinabalu, Borneo. *Journal of Ecology* **99**: 849–857.

Hidaka A, Kitayama K. 2013. Relationship between photosynthetic phosphorus-use efficiency and foliar phosphorus fractions in tropical tree species. *Ecology and Evolution* **3**: 4872–4880.

Hooda N, Weston CJ. 1999. Influence of site and fertiliser addition on nutrient cycling in Eucalyptus globulus plantation in Gippsland, south-eastern Australia. I. Foliage and litter quality. *Australian Journal of Botany* **47**: 189–206.

Hovenden MJ, Leuzinger S, Newton PCD, Fletcher A, Fatichi S, Luscher A, Reich PB, Andresen LC, Beier C, Blumenthal DM *et al.* 2019. Globally consistent influences of seasonal precipitation limit grassland biomass response to elevated CO_2. *Nature Plants* **5**: 167–173.

Ji FJ, Li F, Hao DL, Shiklomanov AN, Yang X, Townsend PA, Dashti H, Nakaji T, Kovach KR, Liu HR *et al.* 2024. Unveiling the transferability of PLSR models for leaf trait estimation: lessons from a comprehensive analysis with a novel global dataset. *New Phytologist* **243**: 111–131.

Jiang MK, Caldararu S, Zaehle S, Ellsworth DS, Medlyn BE. 2019. Towards a more physiological representation of vegetation phosphorus processes in land surface models. *New Phytologist* **222**: 1223–1229.

Jiang MK, Medlyn BE, Wårlind D, Knauer J, Fleischer K, Goll DS, Olin S, Yang XJ, Yu L, Zaehle S *et al.* 2024. Carbon-phosphorus cycle models overestimate CO_2 enrichment response in a mature Eucalyptus forest. *Science Advances* **10**: eadl5822.

Jin Y, Qian H. 2019. V.PhyloMaker: an R package that can generate very large phylogenies for vascular plants. *Ecography* **42**: 1353–1359.

Kedrowski RA. 1983. Extraction and analysis of nitrogen, phosphorus and carbon fractions in plant-material. *Journal of Plant Nutrition* **6**: 989–1011.

Kembel SW, Cowan PD, Helmus MR, Cornwell WK, Morlon H, Ackerly DD, Blomberg SP, Webb CO. 2010. Picante: R tools for integrating phylogenies and ecology. *Bioinformatics* **26**: 1463–1464.

Kokaly RF, Asner GP, Ollinger SV, Martin ME, Wessman CA. 2009. Characterizing canopy biochemistry from imaging spectroscopy and its application to ecosystem studies. *Remote Sensing of Environment* **113**: S78–S91.

Kothari S, Beauchamp-Rioux R, Blanchard F, Crofts AL, Girard A, Guilbeault-Mayers X, Hacker PW, Pardo J, Schweiger AK, Demers-Thibeault S *et al.* 2023b. Predicting leaf traits across functional groups using reflectance spectroscopy. *New Phytologist* **238**: 549–566.

Kothari S, Beauchamp-Rioux R, Laliberté E, Cavender-Bares J. 2023a. Reflectance spectroscopy allows rapid, accurate and non-destructive estimates of functional traits from pressed leaves. *Methods in Ecology and Evolution* **14**: 385–401.

Lagace TA, Ridgway ND. 2013. The role of phospholipids in the biological activity and structure of the endoplasmic reticulum. *Biochimica et Biophysica Acta, Molecular Cell Research* **1833**: 2499–2510.

Lambers H. 2022. Phosphorus acquisition and utilization in plants. *Annual Review of Plant Biology* **73**: 17–42.

Lambers H, Cawthray GR, Giavalisco P, Kuo J, Laliberté E, Pearse SJ, Scheible WR, Stitt M, Teste F, Turner BL. 2012. Proteaceae from severely phosphorus-impoverished soils extensively replace phospholipids with galactolipids and sulfolipids during leaf development to achieve a high photosynthetic phosphorus-use-efficiency. *New Phytologist* **196**: 1098–1108.

Lambers H, Poorter H. 1992. Inherent variation in growth rate between higher plants: a search for physiological causes and ecological consequences. *Advances in Ecological Research* **23**: 187–261.

Lamour J, Davidson KJ, Ely KS, Le Moguédec G, Anderson JA, Li QY, Calderón O, Koven CD, Wright SJ, Walker AP *et al.* 2023. The effect of the vertical gradients of photosynthetic parameters on the CO_2 assimilation and transpiration of a Panamanian tropical forest. *New Phytologist* **238**: 2345–2362.

Liang GH, Butler OM, Warren CR. 2024. Lipid profiles of plants and soil microbial communities are shaped by soil parent material in Australian sclerophyll forests. *Plant and Soil* **498**: 39–55.

Liu NF, Hokanson EW, Hansen H, Townsend PA. 2023. Multi-year hyperspectral remote sensing of a comprehensive set of crop foliar nutrients in cranberries. *ISPRS Journal of Photogrammetry and Remote Sensing* **205**: 135–146.

Liu ST, Gille CE, Bird T, Ranathunge K, Finnegan PM, Lambers H. 2023. Leaf phosphorus allocation to chemical fractions and its seasonal variation in south-western Australia is a species-dependent trait. *Science of the Total Environment* **901**: 166395.

Liu SW, Yan ZB, Wang ZH, Serbin SP, Visser M, Zeng Y, Ryu Y, Su YJ, Guo ZF, Song GQ *et al.* 2023. Mapping foliar photosynthetic capacity in sub-tropical and tropical forests with UAS-based imaging spectroscopy: scaling from leaf to canopy. *Remote Sensing of Environment* **293**: 113612.

Liu SW, Wang ZH, Lin ZY, Zhao YY, Yan ZB, Zhang K, Visser M, Townsend PA, Wu J. 2023. Spectra-phenology integration for high-resolution, accurate, and scalable mapping of foliar functional traits using time-series Sentinel-2 data. *Remote Sensing of Environment* **305**: 114082.

Martin ME, Plourde LC, Ollinger SV, Smith ML, McNeil BE. 2008. A generalizable method for remote sensing of canopy nitrogen across a wide range of forest ecosystems. *Remote Sensing of Environment* **112**: 3511–3519.

Meng QQ, Shi ZJ, Yan ZB, Lambers H, Luo Y, Han WX. 2025. Independent and interactive effects of N and P additions on foliar P fractions in evergreen forests of southern China. *Forest Ecosystems* **12**: 100265.

Mimura T, Sakano K, Shimmen T. 1996. Studies on the distribution, retranslocation and homeostasis of inorganic phosphate in barley leaves. *Plant, Cell & Environment* **19**: 311–320.

Mo Q, Li ZA, Sayer EJ, Lambers H, Li Y, Zou B, Tang J, Heskel M, Ding Y. 2019. Foliar phosphorus fractions reveal how tropical plants maintain photosynthetic rates despite low soil phosphorus availability. *Functional Ecology* **33**: 503–513.

Nunes MH, Davey MP, Coomes DA. 2017. On the challenges of using field spectroscopy to measure the impact of soil type on leaf traits. *Biogeosciences* **14**: 3371–3385.

Ollinger SV. 2011. Sources of variability in canopy reflectance and the convergent properties of plants. *New Phytologist* **189**: 375–394.

Ostertag R. 2010. Foliar nitrogen and phosphorus accumulation responses after fertilization: an example from nutrient-limited Hawaiian forests. *Plant and Soil* **334**: 85–98.

Pagel M. 1999. Inferring the historical patterns of biological evolution. *Nature* **401**: 877–884.

Pedregosa F, Varoquaux G, Gramfort A, Michel V, Thirion B, Grisel O, Blondel M, Prettenhofer P, Weiss R, Dubourg V *et al.* 2011. Scikit-learn: machine learning in Python. *Journal of Machine Learning Research* **12**: 2825–2830.

Poirier Y, Jaskolowski A, Clúa J. 2022. Phosphate acquisition and metabolism in plants. *Current Biology* **32**: 589–683.

Reich PB, Walters MB, Ellsworth DS. 1997. From tropics to tundra: global convergence in plant functioning. *Proceedings of the National Academy of Sciences, USA* **94**: 13730–13734.

Reich PB, Wright IJ, Lusk CH. 2007. Predicting leaf physiology from simple plant and climate attributes: a global GLOPNET analysis. *Ecological Applications* **17**: 1982–1988.

Rogers A, Serbin SP, Ely KS, Sloan VL, Wullschleger SD. 2017. Terrestrial biosphere models underestimate photosynthetic capacity and CO_2 assimilation in the Arctic. *New Phytologist* **216**: 1090–1103.

Rowland L, Zaragoza-Castells J, Bloomfield KJ, Turnbull MH, Bonal D, Burban B, Salinas N, Cosio E, Metcalfe DJ, Ford A *et al.* 2016. Scaling leaf respiration with nitrogen and phosphorus in tropical forests across two continents. *New Phytologist* **214**: 903–904.

Schweiger AH, Schweiger JMI. 2024. Significant links between photosynthetic capacity, atmospheric CO_2 and the diversification of C_3 plants during the last 80 million years. *Ecology Letters* **27**: e14523.

Serbin SP, Singh A, McNeil BE, Kingdon CC, Townsend PA. 2014. Spectroscopic determination of leaf morphological and biochemical traits for northern temperate and boreal tree species. *Ecological Applications* **24**: 1651–1669.

Serbin SP, Townsend PA. 2020. Scaling functional traits from leaves to canopies. In: Cavender-Bares J, Gamon JA, Townsend PA, eds. *Remote sensing of plant biodiversity*. Cham, Switzerland: Springer, 43–82.

Serbin SP, Wu J, Ely KS, Kruger EL, Townsend PA, Meng R, Wolfe BT, Chlus A, Wang ZH, Rogers A. 2019. From the Arctic to the tropics: multibiome prediction of leaf mass per area using leaf reflectance. *New Phytologist* **224**: 1557–1568.

Sperry J. 2013. Cutting-edge research or cutting-edge artefact? An overdue control experiment complicates the xylem refilling story. *Plant, Cell & Environment* **36**: 1916–1918.

Sterner RW, Elser JJ. 2002. Biological chemistry: building cells from elements. In: Sterner RW, Elser JJ, eds. *Ecological stoichiometry: the biology of elements from molecules to the biosphere*. Princeton, NJ, USA: Princeton University Press, 44–79.

Sulpice R, Ishihara H, Schlereth A, Cawthray GR, Encke B, Giavalisco P, Ivakov A,Arrivault S, Jost R, Krohn N *et al.* 2014. Low levels of ribosomal RNA partlyaccount for the very high photosynthetic phosphorus-use efficiency of Proteaceaespecies. *Plant, Cell & Environment* **37**: 1276–1298.

Suriyagoda LDB, Ryan MH, Gille CE, Dayrell RLC, Finnegan PM, Ranathunge K, Nicol D, Lambers H. 2022. Phosphorus fractions in leaves. *New Phytologist* **237**: 1122–1135.

Swenson NG. 2014. Phylogenetic diversity. In: Swenson NG, ed. *Functional and phylogenetic ecology in R*. New York, NJ, USA: Springer, 27–55.

Swenson NG. 2019. Introduction and a brief phylogenetics primer. In: Swenson NG, ed. *Phylogenetic ecology: a history, critique, and remodeling*. Chicago, IL, USA: University of Chicago Press, 1–19.

Thornley JHM, Cannell MGR. 2000. Modelling the components of plant respiration: representation and realism. *Annals of Botany* **85**: 937.

Tsujii Y, Atwell BJ, Lambers H, Wright IJ. 2024. Leaf phosphorus fractions vary with leaf economic traits among 35 Australian woody species. *New Phytologist* **241**: 1985–1997.

Tsujii Y, Fan BL, Atwell BJ, Lambers H, Lei ZY, Wright IJ. 2023. A survey of leaf phosphorus fractions and leaf economic traits among 12 co-occurring woody species on phosphorus-impoverished soils. *Plant and Soil* **489**: 107–124.

Tsujii Y, Onoda Y, Kitayama K. 2017. Phosphorus and nitrogen resorption from different chemical fractions in senescing leaves of tropical tree species on Mount Kinabalu, Borneo. *Oecologia* **185**: 171–180.

Ustin SL, Gitelson AA, Jacquemoud S, Schaepman M, Asner GP, Gamon JA, Zarco-Tejada P. 2009. Retrieval of foliar information about plant pigment systems from high resolution spectroscopy. *Remote Sensing of Environment* **113**: S67–S77.

Veneklaas EJ, Lambers H, Bragg J, Finnegan PM, Lovelock CE, Plaxton WC, Price CA, Scheible WR, Shane MW, White PJ *et al.* 2012. Opportunities for improving phosphorus-use efficiency in crop plants. *New Phytologist* **195**: 306–320.

Vitousek PM, Porder S, Houlton BZ, Chadwick OA. 2010. Terrestrial phosphorus limitation: mechanisms, implications, and nitrogen-phosphorus interactions. *Ecological Applications* **20**: 5–15.

Wang ZH, Chlus A, Geygan R, Ye ZW, Zheng T, Singh A, Couture JJ, Cavender-Bares J, Kruger EL, Townsend PA. 2020. Foliar functional traits from imaging spectroscopy across biomes in eastern North America. *New Phytologist* **228**: 494–511.

Wang ZH, Townsend PA, Kruger EL. 2022. Leaf spectroscopy reveals divergent inter- and intra-species foliar trait covariation and trait-environment relationships across NEON domains. *New Phytologist* **235**: 923–938.

Westoby M, Falster DS, Moles AT, Vesk PA, Wright IJ. 2002. Plant ecological strategies: some leading dimensions of variation between species. *Annual Review of Ecology and Systematics* **33**: 125–159.

White PJ, Hammond JP. 2008. Phosphorus nutrition of terrestrial plants. In: White PJ, Hammond JP, eds. *The ecophysiology of plant-phosphorus interactions*. Dordrecht, the Netherlands: Springer, 51–81.

Wijewardane NK, Zhang HC, Yang JL, Schnable JC, Schachtman DP, Ge YF. 2023. A leaf-level spectral library to support high-throughput plant phenotyping: predictive accuracy and model transfer. *Journal of Experimental Botany* **74**: 4050–4062.

Wold S, Sjöström M, Eriksson L. 2001. PLS-regression: a basic tool of chemometrics. *Chemometrics and Intelligent Laboratory Systems* **58**: 109–130.

Wright IJ, Reich PB, Cornelissen JHC, Falster DS, Groom PK, Hikosaka K, Lee W, Lusk CH, Niinemets U, Oleksyn J *et al.* 2005. Modulation of leaf economic traits and trait relationships by climate. *Global Ecology and Biogeography* **14**: 411–421.

Wright IJ, Reich PB, Westoby M, Ackerly DD, Baruch Z, Bongers F, Cavender-Bares J, Chapin T, Cornelissen JHC, Diemer M *et al.* 2004. The worldwide leaf economics spectrum. *Nature* **428**: 821–827.

Wu FQ, Liu SW, Lamour J, Atkin OK, Yang N, Dong TT, Xu WY, Smith NG, Wang ZH, Wang H *et al.* 2025. Linking leaf dark respiration to leaf traits and reflectance spectroscopy across diverse forest types. *New Phytologist* **246**: 481–497.

Wu J, Rogers A, Albert LP, Ely K, Prohaska N, Wolfe BT, Oliveira RC Jr, Saleska SR, Serbin SP. 2019. Leaf reflectance spectroscopy captures variation in carboxylation capacity across species, canopy environment and leaf age in lowland moist tropical forests. *New Phytologist* **224**: 663–674.

Yan L, Sunoj VSJ, Short AW, Lambers H, Elsheery NI, Kajita T, Wee AKS, Cao KF. 2021. Correlations between allocation to foliar phosphorus fractions and maintenance of photosynthetic integrity in six mangrove populations as affected by chilling. *New Phytologist* **232**: 2267–2282.

Yan L, Zhang XH, Han ZM, Pang JY, Lambers H, Finnegan PM. 2019. Responses of foliar phosphorus fractions to soil age are diverse along a 2 Myr dune chronosequence. *New Phytologist* **223**: 1621–1633.

Yan ZB, Guo ZF, Serbin SP, Song GQ, Zhao YY, Chen Y, Wu SB, Wang J, Wang X, Li J *et al.* 2021. Spectroscopy outperforms leaf trait relationships for predicting photosynthetic capacity across different forest types. *New Phytologist* **232**: 134–147.

Yan ZB, Sardans J, Peñuelas J, Detto M, Smith NG, Wang H, Guo LL, Hughes AC, Guo ZF, Lee CKF *et al.* 2023. Global patterns and drivers of leaf photosynthetic capacity: the relative importance of environmental factors and evolutionary history. *Global Ecology and Biogeography* **32**: 668–682.

Zhang GH, Zhang LL, Wen DZ. 2018. Photosynthesis of subtropical forest species from different successional status in relation to foliar nutrients and phosphorus fractions. *Scientific Reports* **8**: 10455.

Supporting Information

Additional Supporting Information may be found online in the Supporting Information section at the end of the article.

Fig. S1 Variance partitioning of leaf phosphorus (P) fractions within and across forest sites.

Fig. S2 Phylogenetic structure of leaf phosphorus (P) fractions across forest types.

Fig. S3 Variation in leaf morphological and biochemical traits across forest types.

Fig. S4 Variation in leaf photosynthetic traits across forest types.

Fig. S5 Accuracy assessment for the prediction of leaf P concentration ([P]) using leaf reflectance spectroscopy.

Fig. S6 Coefficients of partial least-squares regression that were used to identify the sensitive spectral domains for the spectral modeling of leaf P concentration ([P]) and leaf P fractions.

Methods S1 Protocol of the measurement of A–C_i curves.

Methods S2 Protocol of the measurement of leaf phosphorus (P) fractions.

Methods S3 Protocol of the measurement of leaf biochemical and morphological traits.

Methods S4 Protocol for the development of spectral models in predicting leaf phosphorus (P) fractions across forest types.

Table S1 Soil nutrient characteristics of the three forest types in China.

Table S2 Summary of species, the concentrations of leaf phosphorus (P) fractions and sample size of representative canopy trees across forest types in China.

Table S3 Summary of species and the proportions of leaf phosphorus (P) fractions of representative canopy trees across forest types in China.

Table S4 Summary of species, leaf morphological and biochemical traits of representative canopy trees across forest types in China.

Table S5 Summary of species and leaf photosynthetic traits of representative canopy trees across forest types in China.

Table S6 Results from Pearson's correlations between the concentrations of leaf phosphorus (P) fractions and associated leaf traits across forest types in China.

Table S7 Results from Pearson's correlations between the proportions of leaf phosphorus (P) fractions and associated leaf traits across forest types in China.

Please note: Wiley is not responsible for the content or functionality of any Supporting Information supplied by the authors. Any queries (other than missing material) should be directed to the *New Phytologist* Central Office.